ADVANCED FUNCTIONAL MATERIALS
www.afm-journal.de

Magnetic Assembly of Soft Robots with Hard Components

*Sen W. Kwok, Stephen A. Morin, Bobak Mosadegh, Ju-Hee So, Robert F. Shepherd, Ramses V. Martinez, Barbara Smith, Felice C. Simeone, Adam A. Stokes, and George M. Whitesides**

This paper describes the modular magnetic assembly of reconfigurable, pneumatically actuated robots composed of soft and hard components and materials. The soft components of these hybrid robots are actuators fabricated from silicone elastomers using soft lithography, and the hard components are acrylonitrile–butadiene–styrene (ABS) structures made using 3D printing. Neodymium–iron–boron (NdFeB) ring magnets are embedded in these components to make and maintain the connections between components. The reversibility of these magnetic connections allows the rapid reconfiguration of these robots using components made of different materials (soft and hard) that also have different sizes, structures, and functions; in addition, it accelerates the testing of new designs, the exploration of new capabilities, and the repair or replacement of damaged parts. This method of assembling soft actuators to build soft machines addresses some limitations associated with using soft lithography for the direct molding of complex 3D pneumatic networks. Combining the self-aligning property of magnets with pneumatic control makes it possible for a teleoperator to modify the structures and capabilities of these robots readily in response to the requirements of different tasks.

1. Introduction

Interest in bio-mimetic robots (e.g., flying insects,[1] caterpillar,[2] earthworms,[3] octopi,[4] and jellyfish[5]) has led to rapid development of a new class of robots that exploit magnetic,[6] electrical,[7] thermal,[8] chemical,[9] and mechanical[10,11] properties of soft materials for unconventional strategies of actuation and control. Soft robots and machines (e.g., grippers,[12] tentacles,[13] walkers,[14] rollers,[15,16] and swimmers[17]) fabricated from elastomers, or from composites based on them[18] using soft lithography have demonstrated that a wide range of functions and capabilities—compliant gripping,[12] sampling and delivery of fluids,[13] visualization,[19,20] multi-spectral camouflage,[20] jumping,[21] and multi-modal locomotion[14,22]—can be realized through the use of microfluidics in robotic design.

Previously reported soft robots and machines have not been reconfigurable: Their structures, once generated, were fixed and not amenable to reversible changes that modify capabilities. In addition, devices that are composed of multiple materials and contain networks of channels perpendicular to each other vertically and horizontally can be exceedingly difficult to produce in single step; soft lithography—an efficient technique for rapid prototyping and replication of planar and quasi-two-dimensional elastomeric structures—is insufficient to tackle all challenges associated with the fabrication of complex 3D microfluidic networks in advanced systems. As such, methods that impart re-configurability, simplify the fabrication of actuators with complex designs, or facilitate the integration of non-elastomeric materials (e.g., metals, thermoplastics) and electronics (e.g. sensors and communication units) will greatly accelerate the development of soft robotics.

Reversible modular assembly has been a widely used strategy for fabricating complex hard robots as it enables reconfiguration to suit new tasks, rapid testing of new designs, and easy repair and replacement of damaged parts. This strategy, together with advances in the fabrication and miniaturization of sensors, actuators, power sources, and units for control and communications, has led to the emergence of autonomous, compact hard robots capable of self-assembly[23] and self-reconfiguration.[24,25] Although inter-modular connections made from mechanical joinery (e.g., hooks-and-grooves interlock[23]) are sturdy and reversible, they require either manual orientation and assembly, or the precise alignment for docking of the matching pieces; the latter necessitates the use of elaborate systems of sensors, with feedback and control, for the remote or automated assembly and disassembly of the components.[23] In contrast, magnetic connectors can self-align and assemble;[26–28] hence, they relieve the need for precise spatial control in assembling two complementary units, while preserving the strength and reversibility of mechanical connectors.

This paper describes the modular assembly of hybrid[29] reconfigurable robots/machines using magnets. Although

Dr. S. W. Kwok, Dr. S. A. Morin, Dr. B. Mosadegh, Dr. J.-H. So, Dr. R. F. Shepherd, Dr. R. V. Martinez, Dr. B. Smith, Dr. F. C. Simeone, Dr. A. A. Stokes, Prof. G. M. Whitesides
Department of Chemistry and Chemical Biology
Harvard University
12 Oxford Street, Cambridge, MA, 02138, USA
E-mail: gwhitesides@gmwgroup.harvard. edu
B. Modasegh, G. M. Whitesides
Wyss Institute for Biologically Inspired Engineering
Harvard University
60 Oxford Street, Cambridge, MA 02138, USA

DOI: 10.1002/adfm.201303047

non-magnetic, modular assembly of soft robotic snakes has been explored by Onal et al.,[30] the reconfigurability of the reported robots has not been demonstrated. In the following study, our hybrid robots were assembled from two types of modules—soft actuators (e.g., grippers, legs, tentacles) fabricated from elastomers using soft lithography, and hard scaffolds and connectors (e.g., frame and containers) made of acrylonitirile-butadiene-styrene (ABS) thermoplastics using 3D printing. We embedded neodymium-iron-boron (NdFeB) ring magnets in these actuators and structural elements to connect them, and to maintain the integrity of the assembly. These connections could be reversibly assembled by hand, or modified by a teleoperator using pneumatic controls. Using our approach, we assembled multi-functional, difficult-to-mold hybrid robots (e.g., the robots what we call "surveyor" and "porter" in the following) from soft actuators that are easy to make structures, and combined with hard structural elements.

2. Design and Fabrication of the Soft Robots

2.1. Design and Fabrication of Soft Actuators

We adopted the basic design of the pneumatic networks described in our previous reports,[12–14] and fabricated soft actuators (e.g., legs, grippers, tentacles) using soft lithography. The molds required for these procedures were made of ABS thermoplastics, and prepared using 3D printing. We poured the liquid prepolymer into the fabricated mold, degassed to remove bubbles, and thermally cured it. To introduce a magnetic interface into a soft actuator, we embedded a magnet of appropriate size, with correct orientation of the magnetic pole, into the actuator, and sealed the magnet with silicone elastomer (see the Supporting Information (S.I.) for a detailed description of their fabrication).

2.2. Actuation of Soft Robots

We actuated the soft modules by pressurizing the hollow chamber of the pneumatic network (which we and others call "pneu-nets") with air, which has negligible contribution to the overall mass of the robots and minimizes the burden of mass required to be moved during actuation. To simplify the coordination and timing of actuation necessary for the locomotion of quadrupeds or multi-legged robots, we connected the air inlets of these robots to compressed air source gated by computer-controlled solenoid valves, and programmed the opening and closing of these valves to pressurize each pneu-net (or soft leg) according to the sequences described in our previous reports.[14,20]

2.3. Design and Fabrication of Hard Components

We used 3D printing for prototyping the hard modules from ABS thermoplastics because it enables the rapid fabrication of 3D structures with complicated internal networks of pneumatic channels, and structural supports. Although the entire hard body is printable as a monolithic structure, we chose to assemble the hard bodies of these robots manually from individual hard components using mechanical or magnetic connectors (see S.I.). This strategy accelerated 1) the testing of designs, 2) the replacement of damaged components with new parts, and 3) the removal of non-essential units for a particular task to maximize the power-to-weight ratio of the robot.

2.4. Design of Magnetic Connectors and Choice of Magnets

We chose to use NdFeB ring magnet in our designs (**Figure 1**a–c), rather than magnets of other geometries, because the hollow center of a ring magnet self-aligns with that of other ring magnets of the same inner and outer diameters. Open channels passing through the axially aligned ring magnets then form a continuous conduit for transporting fluid (e.g., air and other gases in the designs described here, but liquids in other designs) between the modules (Figure 1d,e); these fluids can be used for actuation, sampling, and delivery of chemicals. We used NdFeB magnets because they have the highest remanence per unit mass among all permanent magnets that are

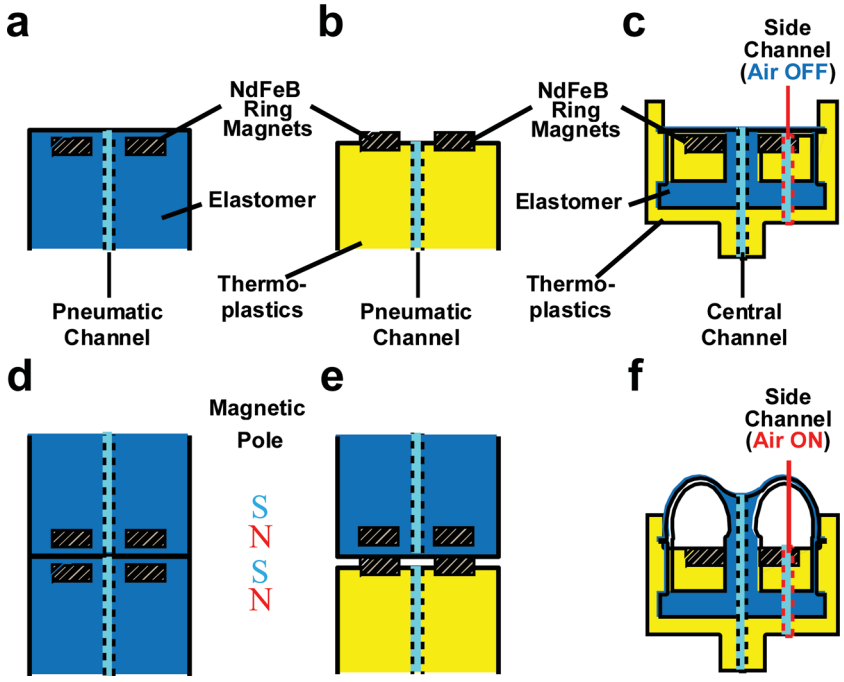

Figure 1. Basic design of magnetic connectors: (a) a soft connector, (b) a hard connector, and (c) a hybrid inflatable connector. Each connector contains a NdFeB ring magnet and a pneumatic channel passing through the center of the embedded magnet. Self-alignment of the hollow centers of the ring magnets forms a continuous conduit between modules. (d) Alignment of two soft modules by the magnetic fields. (e) Alignment of a soft and a hard module. (f) Pneumatic actuation of the integrated bladder of an inflatable connector (c) via the side channel.

commercially available, and are commercially available in many geometries. Using NdFeB magnets maximizes the strength of connection, while minimizing the mass of the assembled device. Electromagnets could, in principle, be used; however, they would be too complex for our current intended uses as they require a supply of electrical current, and additional circuitry, to maintain or alter the connectivity of an assembly.

2.5. Design of Inflatable Connector for Pneumatic Disassembly of Modules

We designed and integrated a pneumatic trigger into the magnetic connectors for remote disassembly of modules (Figure 1c). The capability to disconnect modules remotely provides a teleoperator additional flexibility in tailoring the functions of assembled robots or machines in response to the requirement of a specific job.

Our strategy for disassembly of magnetically assembled components was to inflate a bladder sandwiched between two components. We used pneumatics for disassembly because it could be readily implemented into our existing soft-actuator designs, which also utilized pressurized air for actuation. The side channel of the connector delivered pressurized gas to inflate the bladder (Figure 1f), while the central channel connected and operated the pneumatic network of a magnetically coupled soft actuator (see S.I.). Inflating the bladder increased the distance between two modules and weakened the magnetic force between their embedded magnets. At some distance of separation of the magnets (here, ~1.3 cm), torque—from gravity—overcame the weakened magnetic attraction and disconnected the two adjoining units.

2.6. Determining Tensile and Shear Strengths of Magnetic Connectors

We performed uniaxial pull-force measurements (see S.I.) to determine the attraction force of different magnetic connections against tensile and shear load. Two modules embedded with ring magnets that had their opposite magnetic poles facing each other were mounted on force-measurement instrument, and aligned parallel to the axis of magnetization (Z-axis) of the ring magnets. Maximum attraction force between the modules was determined as the difference between the highest applied load and the load when magnetic force was negligible (<0.01 N).

3. Results and Discussion

3.1. Determining Magnetic Attraction Force between Magnets against Tensile and Shear Load

We varied the dimensions of the ring magnets and the elasticity of the materials in which they were embedded, and determined the magnetic attraction force between these magnets as a function of displacement parallel (tensile) or perpendicular (shear) to their axes of magnetization (z-axis). The tensile load supported by the magnetic connection between two hard modules

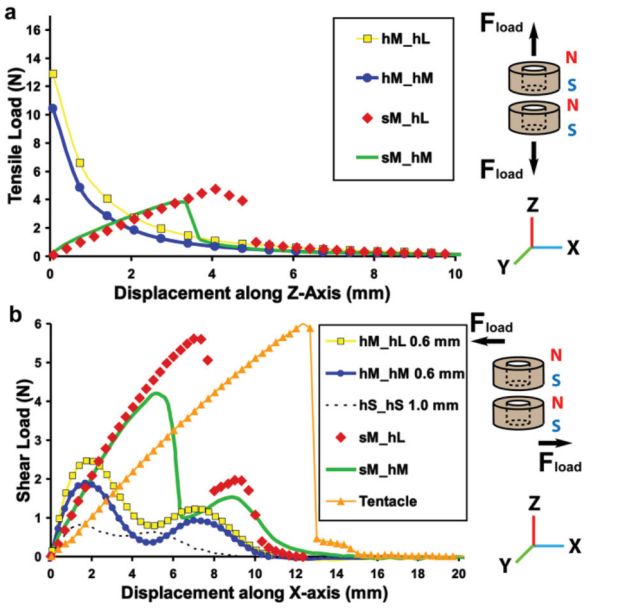

Figure 2. Magnetic attraction force against tensile and shear load as a function of distance of separation between two NdFeB ring magnets. Legends show the various combinations of the magnetic pair used in each measurement. S, M, and L represent ring magnets of the following dimensions (O.D. × I.D. × thickness): 1/4" × 1/8" × 0.1", 3/8" × 1/8" × 0.06", and 3/8" × 1/8" × 0.1" respectively. Prefixes h (hard) and s (soft) indicate the material of the module in which a ring magnet was embedded. Shown on the right of each panel is a simplified schematic of the relative displacement between two magnets under applied load. (a) Magnetic attraction force against tensile load. (b) Magnetic attraction force against shear load. "Tentacle" represents the magnetic connection between a soft tentacle and a hard central connector and it contained four pairs of ring magnets (i.e., 4 × sS_hS).

(graphs of hM_hL and hM_hM, see inset of **Figure 2**a) decayed rapidly with increasing separation (Figure 2a and Figure S16). In contrast, the membrane, (thickness: 0.6–1.0 mm) required to seal the magnet inside of a soft actuator in a soft-hard connection, guaranteed that the two magnets involved in this connection would never be in direct contact, and thus increased the initial separation between the two magnets. As a result, the maximum tensile loads supported by the magnetic attraction forces within soft-hard connections (hM_sL and sM_hM) were similar to that of hard-hard connections separated by an air gap of similar distance (defined by the membrane, 0.6–1.0 mm)—approximately 60% lower than when the two magnets embedded in hard modules were in direct contact (0 mm) (Figure 2a).

The plots of tensile load versus displacement (Figure 2a) in soft-hard connections also had different shape than the equivalent plots of hard-hard connections. In a soft-hard connection, the force initially increased gradually with displacement because the tensile force stretched the soft actuator while the two modules remained in contact. When the applied load exceeded the attractive force for keeping two modules together, the connection severed and the soft module recoiled to its original length. The sudden increase in gap between the magnets led to the rapid reduction of magnetic force that resisted the displacement of the hard module.

In addition to tensile load, we also quantified these magnetic connections against shear load. Similarly to what was observed in the tensile studies, the resistance against shear load decreased rapidly with increasing distance of separation (air gap) between two hard modules (Figure 2b and Figure S17). With an air gap of 0.6 mm (or 1.0 mm), magnets embedded in hard modules, however, showed a 50–60% lower resistance to shear than the same magnetic pair separated by a silicone membrane, instead of air, of similar thickness (0.6–1.0 mm) in a soft-hard connection (Figure 2b). We attributed the higher resistance of soft-hard connection against shear to the friction between the magnet embedded in the hard module and the surface of the soft actuator.

3.2. Magnetic Connections Enable Pneumatic Actuation of Soft Machines Assembled from Soft Actuators

To test whether the magnetic connection was capable of supporting pneumatic actuations of machines assembled from soft modules, we connected two soft actuators (**Figure 3**a), which we called "soft legs", and inserted a poly(ethylene) tube as an air inlet into one of them (Figure 3b). Each leg had an extensible layer and a strain-limiting layer (SLL). Pressurizing the pneumatic channel with air (20–22 kPa) led to preferential expansion of the extensible layer, and caused the anisotropic bending of the legs towards the strain-limiting layers. Actuation of the entire assembly occurred regardless of whether it was suspended vertically or horizontally (Figure 3c–e). These results demonstrated the embedded NdFeB magnets provided a stable connection between two soft legs, and the channels at the hollow centers of the rings formed a well-sealed (but not perfectly sealed), continuous network that supported pneumatic actuation of the assembly. With this proof of concept, we applied this method to assemble soft machines and robots (e.g., a soft tentacle-gripper) that had complex 3D architectures of pneumatic networks, from structurally simpler soft actuators that can be readily fabricated via soft lithography. As an example, we connected a soft tentacle and a soft gripper using magnets (Figure 3f,g and Figure S5,S10 for details of their internal structures); the assembled tentacle-gripper had overhanging pneumatic channels that were difficult to mold in a single step (Figure S11). Pneumatic actuation (38–42 kPa) through the tubing embedded in central channel of the tentacle enabled the vertically-suspended tentacle-gripper to pick up a sphere (weight, 9.5 g) and hold it in the air (Figure 3h–j).

3.3. Reconfiguration and Locomotion of Hybrid Robots

Having demonstrated the ability of our magnetic connection for assembling functional soft machines, we proceeded to apply the design of our magnetic couplers, as demonstrated in soft actuators, to hard structural elements, and combined the resulting hard, magnetic connectors to build hybrid robots made of hard and soft materials. We manually attached the soft legs to the hard magnetic connectors, and used the magnetic attraction between the soft legs and the hard modules to maintain the

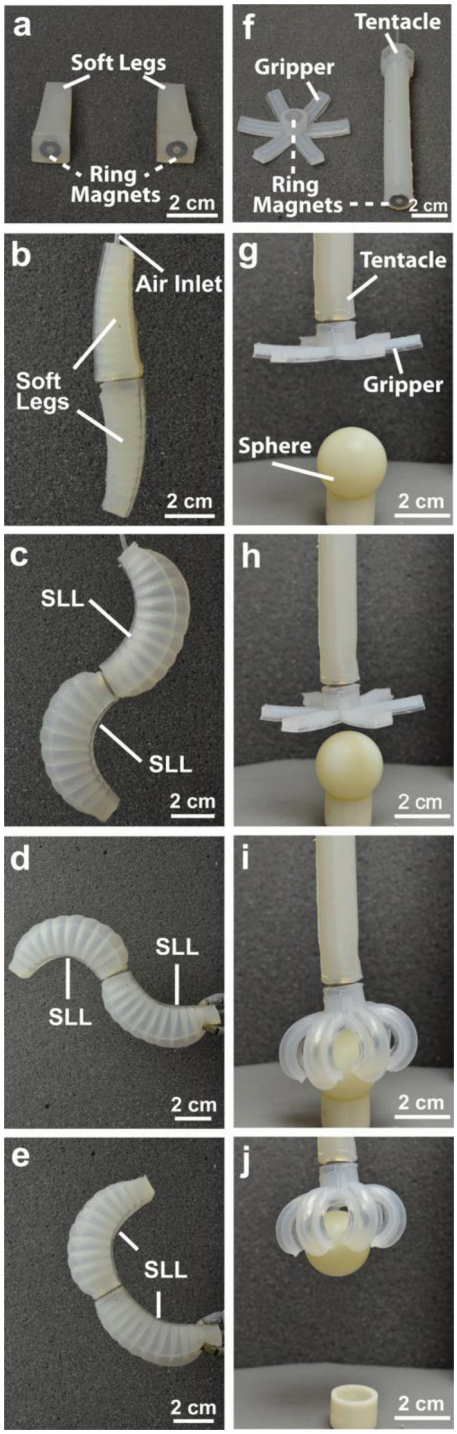

Figure 3. Assembly of soft modules using ring magnets. (a,f) Individual soft actuators before assembly. (b) A vertically suspended assembly of two soft legs, each embedded with the same but oppositely oriented NdFeB ring magnet. (c–e) Pneumatic actuation of an assembly of two soft legs. (c,d) Strain-limiting layers (SLL) located on the opposite face of a (c) vertically and a (d) horizontally suspended assembly. (e) SLL on the same face of an assembly suspended horizontally. (g) A vertically suspended soft machine comprising a soft tentacle and a soft gripper. (h–j) Introducing compressed air through the tubing embedded in the central channel of soft tentacle actuated the magnetically attached gripper to pick up a sphere.

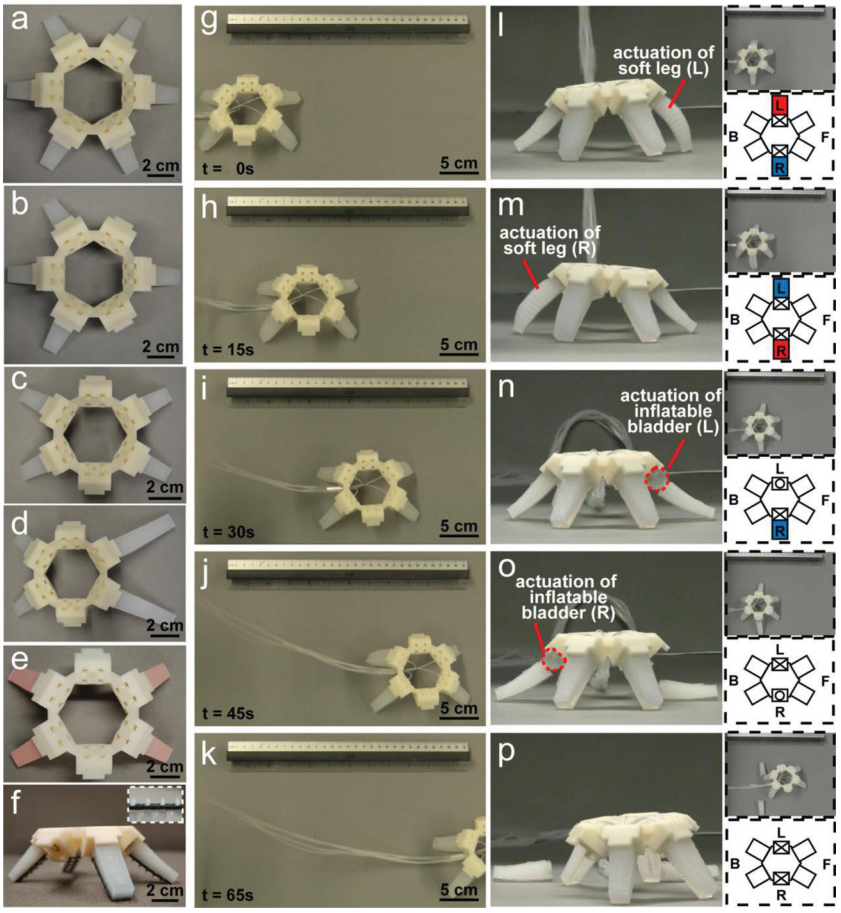

Figure 4. Re-configuration and locomotion of hybrid robots. (a) A hexapedal robot. (b,c) Quadrupeds with different distribution of soft legs around a hexagonal body. (d–f) Quadruped assembled from (d) legs of different sizes, (e) legs made of silicone-paper composite, or (f) legs with spikes. Inset of (f) shows an expanded view of a portion of a spiky leg. (g–k) Locomotion of a tethered hybrid quadruped on a flat, rigid, non-slippery surface. Time (t) is indicated at the bottom left of each panel. (l–p) Locomotion and remote disassembly of a hybrid hexapedal robot. Insets at the top and the bottom right corners of Panels l–p correspond to the top view and the schematic of the state of actuation of the various modules respectively. Soft legs (L and R) in contact with the inflatable connectors are colored: non-actuated states are blue and actuated states are red; these legs were actuated via the central channels of the inflatable connectors. The actuated states of the front and back legs (white rectangular blocks) during locomotion are omitted for clarity. The integrated bladders of the inflatable connectors were pneumatically actuated via the side channels: a cross at the center of small rectangle represents non-actuated state of the integrated bladder while a circle represents its actuated state.

structural integrity of the assembly (**Figure 4**a–f). The reversibility of the magnetic connection allowed the robot to be reconfigured manually, and made it possible to vary the number (Figure 4a,b) and the distribution of soft legs (Figure 4b,c), exchange and combine legs of different size (Figure 4d), material (Figure 4e), and shape (Figure 4f), or replace damaged legs with new ones rapidly.

To test whether the magnetic connections would remain sufficiently stable to support pneumatic actuation of a walking robot, we operated a hybrid quadruped—a robot assembled from four soft legs and a hard body (weighing 63 g, excluding the tethers)—using a computer-controlled compressed air source. Sequential pneumatic actuation[14] of the legs (400 ms actuation at ~50–70 kPa for each leg in every cycle) directed the robot to walk on a flat, rigid, non-slippery surface for a distance of 0.3 m at a speed of ~17 m/h (Figure 4g–k and video S1). The ability of the soft legs to support the continuous movement of the robot highlighted the stability of these magnetic connections in meeting the mechanical and structural demands associated with locomotion.

To demonstrate the feasibility of modifying the structure of a soft robot using remote control, we replaced two of the hard connectors on the opposite side of the hexaped in Figure 4a with inflatable connectors. We first tested the ability of the inflatable connectors to support actuation of the attached soft legs (L and R) by pressurizing these legs with compressed air delivered through the central channels of the connectors (Figure 4l,m). We then stopped the locomotion of the robots, and actuated the integrated bladders of these connectors via the side channels to detach the two legs (Figure 4n,o). The pneumatically triggered disassembly transformed the hexapedal robot into a pentapedal (Figure 4o), and subsequently into a quadrupedal (Figure 4p), walker without physical contact between the operator and the modules of the robot (Video S2).

3.4. Multifunctional Robot Constructed Using Modular Assembly

One major advantage of modular assembly is the integration of additional modules to provide new capabilities. For instance, a modular hybrid robot—comprising an optical hard/soft sensor, and soft legs for walking—can function as a mobile unit for monitoring its surrounding environment.

To assemble a mobile surveyor, we inserted a small video camera at the top opening of the central channel of a soft tentacle and anchored the base of the flexible optical sensor to the center of a hybrid quadruped (**Figure 5**a,b). The connections between the tentacle and the central hub consisted of four pairs of ring magnets (4 × sS_hS) arranged in C_2 symmetry as shown in Figure 5b. The use of multiple pairs of ring magnets in anisotropic configurations provided a self-checking mechanism for engaging two modules in correct orientation. Apart from the central channel, the tentacle had four independently addressable side channels for pneumatic actuation. Adjusting the internal pressure and the number of actuated side channels enabled a high level of control for bending and rotating the flexible optical sensor (Figure 5c–g and video S3).

Once assembled, the surveyor was directed toward a specific location (Figure 5h–i) to inspect a target. After the robot reached its destination (a Styrofoam cup) (Figure 5j), we

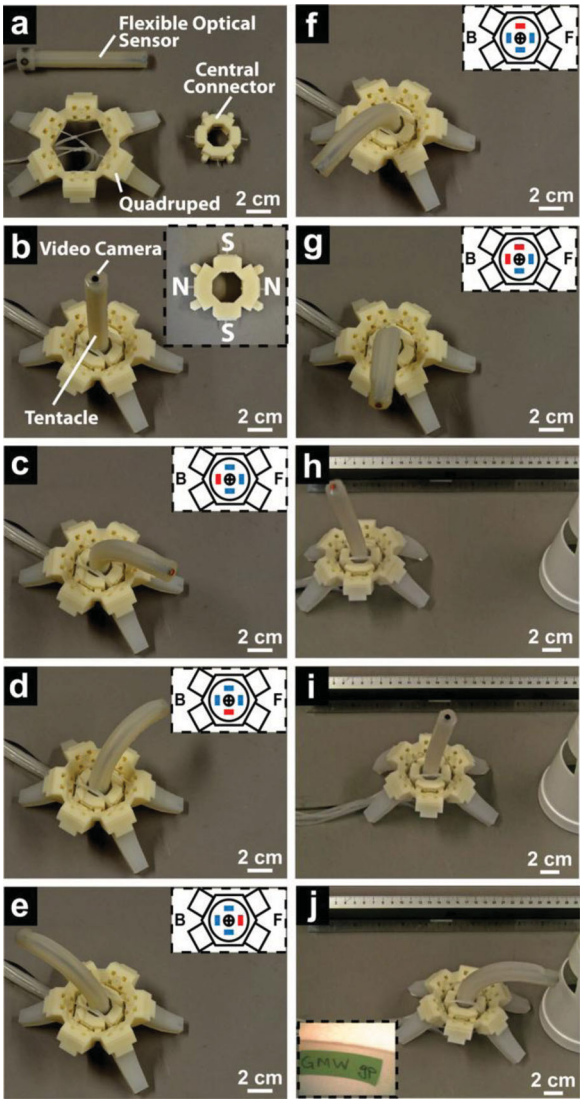

Figure 5. A quadruped walker equipped with a hybrid flexible optical sensor surveys its surrounding environment. Each inset at the top right corner of Panels c–g shows the schematic representation of the state of actuation of the side channels of the soft tentacle. Each colored rectangle represents a side channel: non-actuated channels are blue and actuated channels are red. (a) Modules of a mobile surveyor. (b) An assembled mobile surveyor. Inset of (b) shows the top expanded view of the central connector and the magnetic configuration of the four embedded ring magnets towards the center. (c–f) Inflating a side channel individually caused the tentacle to bend towards the non-actuated channel on the opposite face (maximum degree of bending from the longitudinal axis ~120°). (g) Simultaneous actuation of two neighboring side channels with equal pressure bent the tentacle along the plane bisecting the angle formed between the two channels and the central channel. (h–i) The surveyor moved towards a white Styrofoam cup. (j) Actuation of the soft tentacle positioned the video camera to view the interior of the cup. Bottom left inset of Panel j shows a message, "GMW Gp", hidden inside the cup as viewed from the video camera mounted at the central channel of the soft tentacle.

stopped the actuation of its soft legs. We then actuated the side channels of the soft tentacle to position the camera embedded in the tentacle to view through a window cut into the side wall of the Styrofoam cup; the video camera on the tentacle captured the image of a message, "GMW Gp," hidden inside the container (Figure 5j and Video S3).

3.5. Remote Assembly of Soft Robot Assisted by Self-Alignment of Ring Magnets

The functions and capabilities of earlier examples of robots were constrained by the connectivity of modules that were pre-assembled manually. Although using pneumatically triggered disassembly allows subtractive modification of these robots, a complementary method for remote assembly will significantly expand the number of options available to a teleoperator in adjusting the functions of robots according to the situation.

To test the combination of pneumatic actuators and magnetic connectors for remote assembly of a robot, we equipped a hybrid quadruped with two hard containers, each magnetically coupled to an inflatable connector (**Figure 6**a). This robot, which we called a "porter," was equipped with a left container for carrying a magnet-embedded soft gripper, and a right container that held two spheres to balance the weight of the gripper. A modified soft tentacle with a ring magnet at the apex and a poly(ethylene) tube through the central channel was assembled at the center of the porter.

We directed the robot to walk towards its target (a green sphere) using pneumatic actuation (Figure 6a). Inflating the side channel on the right (Figure 6b) of the soft tentacle pneumatically caused the soft tentacle to bend towards the left container carrying the soft gripper. Attractive magnetic force between the gripper and the magnet at the apex of the bent tentacle pulled the two soft units together at close range, and *self-aligned* the central, open pneumatic channel of the soft tentacle with that of the soft gripper (Video S4).

To test the function of the remotely assembled soft tentacle-gripper in manipulating centimeter-sized object, we used the tentacle to position the gripper above the target (Figure 6c), actuated the gripper to pick up the sphere (Figure 6d), repositioned the gripper with the tentacle using pneumatic control, and released the object into the empty container on the left (Figure 6e). After the robot moved forward over a short distance, we remotely disconnected the magnetically attached containers from the quadruped by inflating the integrated bladders, and thus completed the delivery of its cargo (Figure 6h and Video S4).

4. Conclusions

This work demonstrates the practicality of using magnetic connectors to assemble and disassemble pneumatically actuated soft robots that have components with similar or different material properties (soft and hard), and to assemble those that have complex internal 3D networks of pneumatic channels that are difficult to fabricate as a monolith. These magnetic connections enable rapid, reversible reconfiguration of hybrid soft-hard robots for repair and for testing new designs, and equip these robots with multiple capabilities (e.g., locomotion, surveillance,

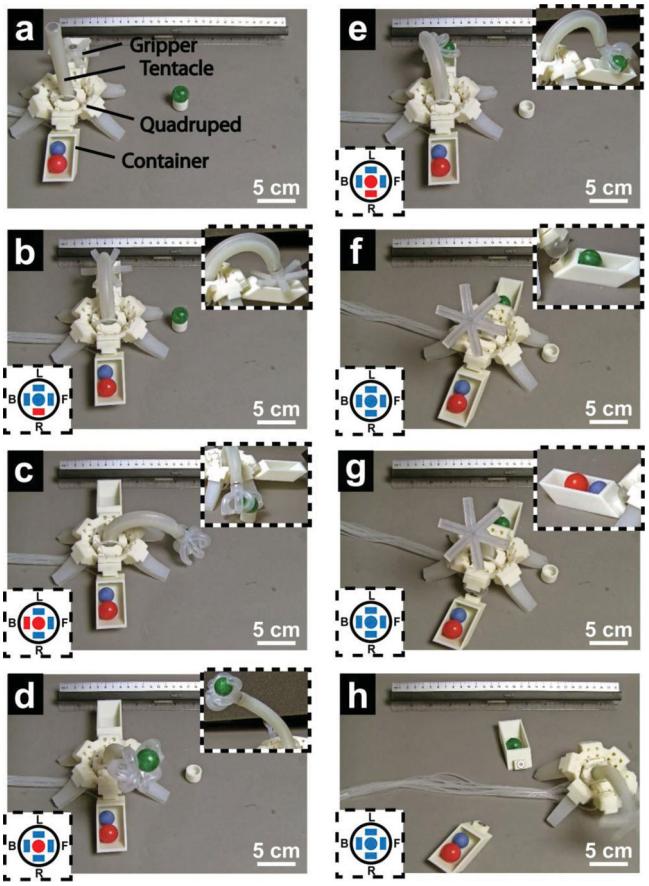

Figure 6. Self-alignment of ring magnets enabled remote assembly of soft actuators, and connection of pneumatic channels for actuation of a soft-hard porter. Panels (a–h) show the top perspective view of the robot. Insets at the bottom left corner of panels (b–h) show the state of actuation of side and central channels of the soft tentacle. The colored circle at the center represents the central channel while each colored rectangle represents one of the four side channels of the soft tentacle. Non-actuated states are blue while actuated states are red. Notations F, B, R, L denote the front, back, right, and left of the robot. Insets at the top right corner of panels (b–g) show the expanded front view of the robot. (a) A pneumatically actuated quadrupedal porter moved towards its target (green sphere). (b) Pneumatically actuated soft tentacle positioned its apex to connect a soft gripper embedded with a ring magnet. (c–e) The assembled tentacle-gripper picked up, and placed the green sphere into the left container for transport. (f,g) After moving forward for a short distance, the robot stopped. Actuation of the inflatable connectors unloaded the cargo together with the containers. (h) Robot continued its forward trajectory after the delivery of cargo had been completed.

and transport and manipulation of centimeter-sized objects). Combining pneumatic actuators and self-aligning magnetic connectors enables a teleoperator to assemble and disassemble more complicated robots on demand. We envision that the capability to modify robots remotely using pneumatics and magnetic connectors will be useful in advancing the design, control, and operation of soft-hard robots and machines (systems that are hybrid of soft and hard components), and provide an alternative to modular assembly using electromagnets or mechanical connectors.

With further development of the control system and power source, and improved design of the soft actuator and magnetic connectors, these modularly assembled hybrid soft-hard robots have the potential to decrease the difficulty, time, and expense of fabrication of soft robots, to enable rapid interchange of components (e.g., legs, tentacles, sensors) to build prototypes and iterate designs, and to repair damaged or defective components.

5. Experimental Section

Please see the Supporting Information.

Supporting Information

Supporting Information is available from the Wiley Online Library or from the author.

Acknowledgements

The design and fabrication of magnetic couplers, and the funding for S.W.K., J.-H.S., and F.C.M. were supported by the US Department of Energy under award DE-FG02-00ER45852. The development of other aspects of the soft machines, and the funding for S.A.M., A.A.S., and R.F.S. were supported by the Defense Advanced Research Planning Agency under award W911NF-11-1-0094. B.M. and B.S.R. acknowledge funding by Wyss Istitute for Biologically-Inspired Engineering at Harvard University. R.V.M. acknowledges funding by the European Commission (FP7 People program) under the project Marie Curie IOF-275148. We thank Dr. James C. Weaver for providing a sample of 3D-printed spikes embedded in an elastomeric sheet, and Mr. Jacob Freake for his initial work on modular assembly of soft robots.

Received: August 31, 2013
Published online: December 11, 2013

[1] K. Y. Ma, P. Chirarattananon, S. B. Fuller, R. J. Wood, *Science* **2013**, *340*, 603.
[2] H.-T. Lin, G. G. Leisk, B. Trimmer, *Bioinspir. Biomim.* **2011**, *6*, 026007.
[3] a) A. Menciassi, S. Gorini, G. Pernorio, P. Dario, in IEEE International Conference on Robotics and Automation, New Orleans, LA, April **2004**, p.3282; b) K. Jung, J. C. Koo, J.-D. Nam, Y. K. Lee, H. R. Choi, *Bioinspir. Biomim.* **2007**, *2*, S42.
[4] a) L. Margheri, C. Laschi, B. Mazzolai, *Bioinspir. Biomim.* **2012**, *7*, 025004; b) B. Mazzolai, L. Margheri, M. Cianchetti, P. Dario, C. Laschi, *Bioinspir. Biomim.* **2012**, *7*, 205005.
[5] J. C. Nawroth, H. Lee, A. W. Feinberg, C. M. Ripplinger, M. L. MaCain, A. Grosberg, J. O. Dabiri, K. K. Parker, *Nat. Biotechnol.* **2012**, *30*, 792.
[6] P. Garstecki, P. Tierno, D. B. Weibel, F. Sagués, G. M. Whitesides, *J. Phys.: Condens. Matter* **2009**, *21*, 204110.
[7] I. A. Anderson, T. A. Gisby, T. G. McKay, B. M. O'Brien, E. P. Calius, *J. Appl. Phys.* **2012**, *112*, 041101.
[8] M. Follador, M. Cianchetti, A. Arienti, C. Laschi, *Smart Mater. Struct.* **2012**, *21*, 115029.
[9] S. Maeda, Y. Hara, T. Sakai, R. Yoshida, S. Hashimoto, *Adv. Mater.* **2007**, *19*, 3480.
[10] C. Keplinger, T. Li, R. Baumgartner, Z. Suo, S. Bauer, *Soft Matter* **2012**, *8*, 285.

[11] E. Brown, N. Rodenberg, J. Amend, A. Mozeika, E. Steltz, M. R. Zakin, H. Lipson, H. M. Jaeger, *Proc. Natl. Acad. Sci. USA* **2010**, *107*, 18809.
[12] F. Ilievski, A. D. Mazzeo, R. F. Shepherd, X. Chen, G. M. Whitesides, *Angew. Chem. Int. Ed.* **2011**, *50*, 1890; *Angew Chem.* **2011**, *123*, 1930.
[13] R. V. Martinez, J. L. Branch, C. R. Fish, L. Jin, R. F. Shepherd, R. M. D. Nunes, Z. Suo, G. M. Whitesides, *Adv. Mater.* **2013**, *25*, 205.
[14] R. F. Shepherd, F. Ilievski, W. Choi, S. A. Morin, A. A. Stokes, A. D. Mazzeo, X. Chen, M. Wang, G. M. Whitesides, *Proc. Natl. Acad. Sci. USA* **2011**, *108*, 20400.
[15] C. D. Onal, X. Chen, G. M. Whitesides, D. Rus, in International Symposium on Robotics Research (ISRR), Flagstaff, Az, USA **2011**.
[16] A. D. Marchese, C. D. Onal, D. Rus, in 2011 IEEE/RSJ International Conference on Intelligent Robots and Systems, San Francisco, CA, USA **2011**, p.756.
[17] K. Suzumori, S. Endo, T. Kanda, N. Kato, H. Suzuki, in IEEE International Conference on Robotics and Automation, Roma, Italy **2007**, p.4975.
[18] R. V. Martinez, C. R. Fish, X. Chen, G. M. Whitesides, *Adv. Funct. Mater.* **2012**, *22*, 1376.
[19] I. Jung, J. Xiao, V. Malyarchuk, C. Lu, M. Li, Z. Liu, J. Yoon, Y. Huang, J. A. Rogers, *Proc. Natl. Acad. Sci. USA* **2011**, *108*, 1788.
[20] S. A. Morin, R. F. Shepherd, S. W. Kwok, A. A. Stokes, A. Nemiroski, G. M. Whitesides, *Science* **2012**, *337*, 828.
[21] R. F. Shepherd, A. A. Stokes, J. Freake, J. Barber, P. W. Snyder, A. D. Mazzeo, L. Cademartiri, S. A. Morin, G. M. Whitesides, *Angew. Chem. Int. Ed.* **2013**, *52*, 1;*Angew. Chem.* **2013**, *125*, 2964.
[22] B. A. Trimmer, H.-T. Lin, A. Baryshyan, G. G. Leisk, D. L. Kaplan, in The Fourth IEEE RAS/EMBS International Conference on Biomedical Robotics and Biomechanics, Roma, Italy, June **2012**, p. 599.
[23] H. Wei, Y. Chen, J. Tan, T. Wang, *IEEE/ASME Transactions on Mechatronics*, **2011**, *16*, 745.
[24] M. Yim, W.-M. Shen, B. Salemi, D. Rus, M. Moll, H. Lipson, E. Klavins, G. S. Chirikjian, in IEEE Robotics & Automation Magazine, **2007**, p.43.
[25] V. Zykov, E. Mytilinaios, B. Adams, H. Lipson, *Nature* **2005**, *435*, 163.
[26] Z. Nagy, R. Oung, J. J. Abbott, B. J. Nelson, *IEEE/RSJ International Conference on Intelligent Robots and Systems*, **2008**, 1915.
[27] M. Boncheva, S. A. Andreev, L. Mahadevan, A. Winkleman, D. R. Reichman, M. G. Prentiss, S. Whitesides, G. M. Whitesides, *Proc. Natl. Acad. Sci. USA* **2005**, *102*, 3924.
[28] C. Pawashe, E. Diller, S. Floyd, M. Sitti, in IEEE International Conference on Robotics and Automation, Shanghai, China **2011**.
[29] A. A. Stokes, R. F. Shepherd, S. A. Morin, F. Ilievski, G. M. Whitesides, *Soft Robotics* **2013**, *1*, 70.
[30] a) C. D. Onal, D. Rus, in The Fourth IEEE RAS/EMBS International Conference on Biomedical Robotics and Biomechantronics, Roma, Italy **2012**, p.1038; b) C. D. Onal, D. Rus, *Bioinspir. Biomim.* **2013**, *8*, 026003.